

Optical measurement of particle size distribution of acoustic cavitation and surrounding sound field

音響キャビテーションの粒度分布とその周辺音場の光学計測

Takanobu Kuroyama^{1†}, Koichi Mizutani^{1*}, Naoto Wakatsuki¹, Tadashi Ebihara¹, and Takeshi Ohbuchi² (¹Univ. of Tsukuba; ²National Defense Academy)

黒山喬允^{1†}, 水谷孝一², 若槻尚斗², 海老原格², 大淵武史³
(¹筑波大院・シス情工, ²筑波大・シス情系, ³防衛大・応物)

1. Introduction

The sonochemical treatment is attracting attentions for its characteristics suitable for wastewater treatment and oxidation of chemicals.¹⁾ For the application of the sonochemical treatment, the measurement of the size distribution of the acoustic cavitation and its surrounding sound field is important to evaluate the effect of the cavitation²⁾ but there are a few reports.

We have been proposed a size distribution measurement method of the cavitation based on the laser diffraction³⁾ and the measurement method of sound field based on the laser deflection⁴⁾. In this paper, the temporal fluctuation of the size distribution of the cavitation and the sound field under the horn are simultaneously measured by combining the authors' proposed methods.

2. Measurement principle

The particle size distribution of the acoustic cavitation and the sound pressure are determined based on the diffracted light measured employing the optical Fourier transform system. Considering the one-dimensional standing ultrasound, the sound pressure, $p(x,t)$, is expressed as,

$$p(x,t) = p_0 \sin(kx + \phi) \sin(\omega t), \quad (1)$$

where p_0 , k , ϕ , and ω are the global sound pressure, the acoustic wavenumber, the initial phase, and the acoustic angular frequency, respectively. Assuming that the Gaussian laser beam passes through the sound field and irradiates the cavitation bubbles as shown in **Fig. 1**, the light intensity on the focal plane of the Fourier transform lens, $I(x,y,t)$, can be approximated by following equations under the conditions that the laser beam diameter, ρ , and the cavitation diameters are significantly smaller than that of laser beam,

$$I(x,y,t) = \begin{cases} \int_0^\infty v(a,t) a^4 J_1(X)^2 / X^2 da & (|y| \gg \frac{6f\lambda}{\rho\pi}) \\ P\pi^2 / (\alpha\beta) G_x(x,t) G_y(y) & (other) \end{cases}, \quad (2)$$

$$X = 2\pi a_n \sqrt{x^2 + y^2} / (\lambda f), \quad (3)$$

$$G_x(x,t) = \exp\{-\rho^2 \pi^2 [x / (\lambda f) - c_1 S \gamma / \lambda]^2 / 2\}, \quad (4)$$

$$G_y(y) = \exp\{-\rho^2 \pi^2 [y / (\lambda f)]^2 / 2\}, \quad (5)$$

$$c_1 = \partial p(x,t) / \partial x = C_1 \sin(\omega t), \quad (6)$$

$$C_1 = k p_0 \cos(kx + \phi), \quad (7)$$

where λ , f , $v(a,t)$, J_1 , S , and γ are the optical wave-

*mizutani@iit.tsukuba.ac.jp

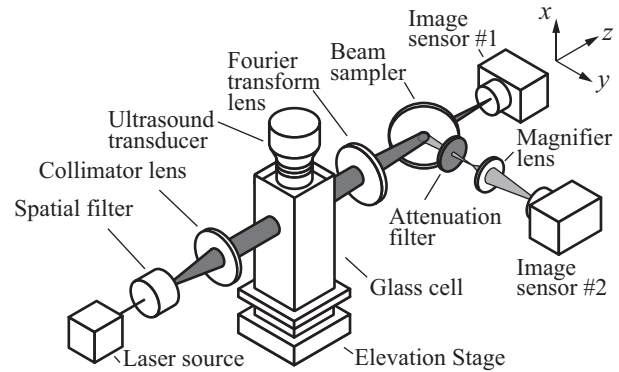


Fig. 1 Experimental system.

length, the focal length of the Fourier transform lens, the volume fraction of the cavitation of diameter, a , (volume based size distribution), the first-order first-kind Bessel function, the path length of the laser beam in the sound field, and the acousto-optic coefficient, respectively.⁴⁾

The light intensity apart from the light axis is dominated by the diffraction caused by the cavitation. The size distribution is determined as $v(a,t)$ minimizing the squared-difference between the theoretical and the measured light intensity.³⁾ The light intensity near the light axis is almost not affected by the cavitation, but mainly affected by the sound. The light intensity near the light axis has the Gaussian profile and that profile is slightly displaced toward x -direction in proportion to the spatial gradient of the sound pressure. The maximal and minimal values of the displacement amplitude, C_1 , correspond to the node and antinode, respectively.⁴⁾

3. Experiments and discussions

Figure 2 shows the experimental system. Ultrasound is irradiated from a bolt-clamped Langevin-type transducer (BLT) with a horn. The horn is immersed into water in a glass cell whose inner cross section is $30 \times 30 \text{ mm}^2$. The BLT is driven by a sinusoidal voltage of 36.3 kHz frequency. The glass cell and the BLT are scanned by a stage to change the laser incident point. The acoustic wavelength is 41.2 mm.

A pulsed laser beam with 640 nm vacuum wavelength and 100 ns duration is spatially filtered and collimated to 5 mm diameter. The pulse timing is synchronized to the phase of the driving voltage of the BLT. The collimated laser beam is incident to the glass cell and the outgoing beam enters a Fourier

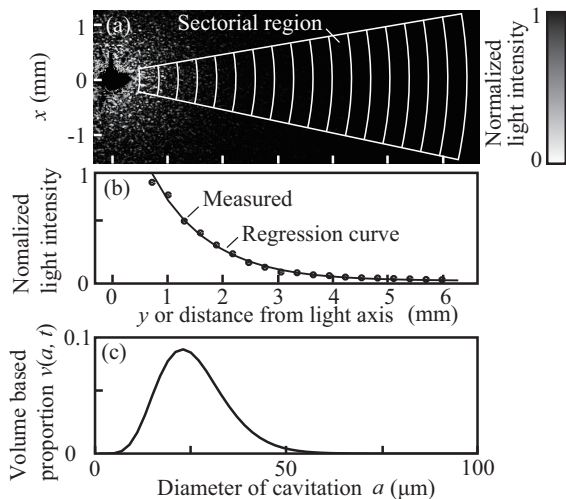


Fig. 2 Diffracted light for determining size distribution (a) Measured image (b) Light intensity averaged in sectorial region and regression curve (c) Size distribution corresponding to regression curve.

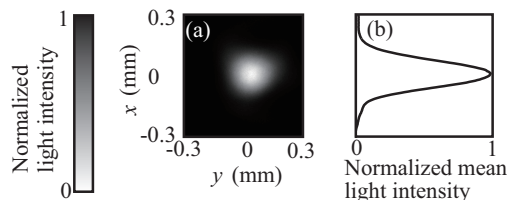


Fig. 3 Gaussian light intensity profile near light axis for determining sound field (a) Measured image (b) Light intensity averaged along y -direction.

transform lens of 200 mm focal length. The convergent beam from the lens is partially reflected by a beam sampler. The transmitted light intensity is measured on the focal plane by an image sensor #1. The reflected light intensity is measured by an image sensor #2 through a magnifier lens. The magnification ratio is 10 and thus the focal length of the Fourier transform lens apparently becomes 2000 mm.

Figure 2(a) shows the typical light intensity measured by the image sensor #1. The background light intensity was independently measured without driving the BLT and canceled. The light intensity near the light axis was missed because of the saturation of the image sensor. **Figure 2(b)** shows the light intensity averaged in the sectorial regions schematically shown in **Fig. 2(a)**. The dashed line is the regression curve. **Fig. 2(c)** shows the determined size distribution corresponding to the regression curve. **Figure 3(a)** shows the typical light intensity near the light axis measured by the image sensor #2. **Figure 3(b)** is the normalized light intensity averaged along the y -axis, which is proportional to the Eq. (4). The displacement amplitude was calculated from this profile.

Figure 4(a) shows the total diffracted light energy apart from the light axis integrated in all the sectorial regions and temporal phase. The larger the energy corresponds to the more amount of the cavitation. Therefore, it was found that the cavitation was distributed near the horn surface. It may be caused that the cavitation was originated from the

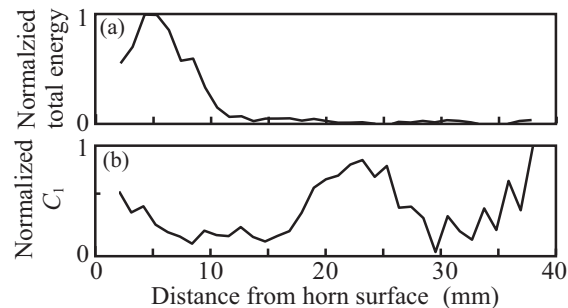


Fig. 4 Spatial distribution of (a) Normalized total energy corresponds to amount of cavitation and (b) Normalized displacement amplitude, C_1 .

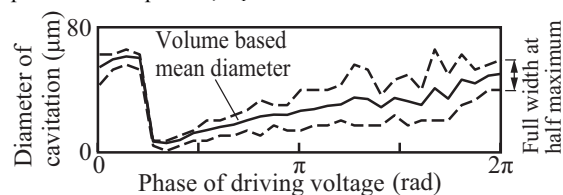


Fig. 5 Temporal fluctuation of the size distribution measured at distance from horn surface is 4 mm.

nuclei on the horn surface and moved toward the focal spot below the horn similar to the cone-like bubble structure.⁶⁾ **Figure 4(b)** shows the normalized displacement amplitude of the Gaussian profile. The minimal points around the distances from the surface, δ , were 10 and 32 (mm) corresponded to the pressure antinode. The interval between these nodes was about 22 mm, which closed to the half acoustic wavelength (20.6 mm).

Figure 5 shows the temporal fluctuation of the size distribution of the cavitation at $\delta = 4$ mm. The diameter periodically increased and decreased depending on the phase of BLT driving voltage. The increasing rate was relatively slow and the decreasing rate was fast like the single bubble oscillation⁵⁾. Therefore, the cavitation originated from the nuclei on the horn surface actively oscillated and were distributed between the horn surface and the first pressure antinode.

4. Conclusion

The size distribution of the cavitation and the sound field were simultaneously measured employing the proposed method. It was revealed that the temporal fluctuation of the size distribution of the cavitation, which was distributed between the horn surface and the first pressure antinode under the horn.

Acknowledgment

This work is supported by a Grant-in Aid for JSPS Fellows Number 13J01995.

References

1. C. Honma *et al.*: Jpn. J. Appl. Phys. **52** (2013) 07HE11.
2. T. G. Leighton, Ultrason. Sonochem. **2** (1995) S123.
3. T. Kuroyama *et al.*: Jpn. J. Appl. Phys. **52** (2013) 07HE15.
4. T. Kuroyama *et al.*: Proc. Symp. on Ultrason. Elect. **35** (2014) 489.
5. D. F. Gaitan *et al.*: J. Acoust. Soc. Am. **91** (1992) 3166.
6. O. Louisnard: Ultrason. Sonochem. **19** (2012) 66.